Available online at www.sciencedirect.com

ScienceDirect

Procedia Engineering 154 (2016) 959 – 966

Procedia Engineering

www.elsevier.com/locate/procedia

12th International Conference on Hydroinformatics, HIC 2016

Evaluation of Plane Wave Assumption in Transient Laminar Pipe Flow Modeling and Utilization

Tong-Chuan Che*, Huan-Feng Duan

Department of Civil and Environmental Engineering, The Hong Kong Polytechnic University, Hung Hom, Kowloon 999077, Hong Kong

Abstract

The plane wave assumption is key to the formulation of one dimensional (1D) and quasi-2D water hammer models, which have been widely used in the design and evaluation of fluid piping systems. As transient analysis and utilization are becoming more and more popular and important to pipe system diagnosis such as pipe faults (leakage and blockage) detection, a better understanding of the influence of plane wave assumption on the transient responses is necessary and critical to the development and application of such innovative technologies. This study aims to (i) address the efficiency problem of existing 2D scheme, and then extend the full-2D water hammer model to a classical reservoir-pipe-valve system so as to simulate the whole process of typical water hammer event; and (ii) estimate the accuracy of plane wave assumption for reproducing pressure histories under both low frequency wave (LFW) and high frequency wave (HFW) conditions. The results confirm that the plane wave assumption is invalid during the period shortly after valve closure, and the influence of radial pressure wave is evident when the incident wave frequency is larger than the radial wave frequency. Moreover, the radial wave dissipation and dispersion rates are highly dependent on the incident wave frequency. This result may provide implication to the utilization of different transient waves (LFW & HFW) for the pipeline assessment in this field.

Peer-review under responsibility of the organizing committee of HIC 2016

Keywords: Water hammer; Transient laminar flow; Plane wave assumption; Full-2D model; LFW; HFW.

* Corresponding author. Tel.: +852-6769-5088; fax: +852-2334-6389.
E-mail address: tongchuan.che@polyu.edu.hk (T.C. Che); hf.duan@polyu.edu.hk (H.F. Duan).

Peer-review under responsibility of the organizing committee of HIC 2016
doi:10.1016/j.proeng.2016.07.533

1. Introduction

Water hammer or hydraulic transients are unsteady pressure fluctuations, with high propagation speed (around 1000m/s in elastic pipes), caused by a flow change. Such fluctuations are easily trigged by many planned or accidental changes in urban water supply pipeline systems, e.g. opening or closing valves, starting or stopping pumps, variations in the supply and demand of the water, etc. The traditional application of transient analysis is mainly for the prediction of pressure history in pipe systems under worst-case scenarios to assist the design and evaluation of pipeline strength and transient control devices.

For many years, the one-dimensional (1D) and quasi-2D water hammer models are commonly adopted for the prediction of such pressure history [1,2], in which the radial inertia and viscous terms are negligible in comparison with their axial counterparts (usually referred to as plane wave assumption) due to the slight compressibility of the fluid and the conduit. Many application results have demonstrated the applicability and validity of such plane wave assumption for the transient system design [3,4].

Although the above-mentioned neglected radial terms are sometimes relatively small compared with their axial counterparts, it would be more physically accurate if these terms are included in the water hammer models, such as for the design of protection devices in which the detailed flow process is required to be modeled in addition to pressure head amplitudes. Meanwhile, as the transient analysis and utilization are becoming more and more popular in some sophisticated fields such as pipe defects (leakage, blockage) detection in the literature [5], where the wave propagation details need to be evaluated and analyzed, a better understanding of the influence of plane wave assumption on the transient responses is necessary and critical to the development and application of such innovative technologies. The full-2D water hammer model, which includes all terms neglected in current 1D and quasi-2D models, is a potential tool for such investigation. The complete form of the 2D model was proposed in [6] for the analysis of instantaneous water hammer wave under the condition of valve operation. However, this proposed full-2D model and scheme were only applied to simple valve-pipe system without any reflection boundary due to their limitations in numerical efficiency for simulating the water hammer process of a water supply pipeline system [6].

This study firstly addresses the efficiency problem of existing 2D numerical scheme, which is then modified and extended to a classical pipe-reservoir-valve system for transient laminar pipe flow modeling. The numerical results of the modified full-2D model are compared with the results from the classical model of Zielke, which has been validated by experimental data in the literature [7]. Thereafter, the validity of the plane wave assumption made in current 1D and quasi-2D models under conditions of different wave frequencies, i.e., low frequency wave (LFW) and high frequency wave (HFW) is examined and discussed for transient modeling and utilization.

2. Materials and methods

2.1. Full-2D water hammer model

In order to generalize and simplify the problem, the full-2D Navier-Stokes and continuity equations are written in non-dimensional form [6].

$$\frac{\partial p}{\partial \tau}+\frac{\partial u}{\partial \xi}+\frac{\partial v}{\partial \eta}+\frac{v}{\eta}=-M\left(u\frac{\partial p}{\partial \xi}+v\frac{\partial p}{\partial \eta}\right) \tag{1}$$

$$\frac{\partial u}{\partial \tau}+\frac{\partial p}{\partial \xi}=-M\left(u\frac{\partial u}{\partial \xi}+v\frac{\partial u}{\partial \eta}\right)+H\left[\frac{4}{3}\frac{\partial^2 u}{\partial \xi^2}+\frac{1}{\eta}\frac{\partial}{\partial \eta}\left(\eta\frac{\partial u}{\partial \eta}\right)+\frac{1}{3}\frac{\partial}{\partial \xi}\left(\frac{1}{\eta}\frac{\partial}{\partial \eta}(\eta v)\right)\right] \tag{2}$$

$$\frac{\partial v}{\partial \tau}+\frac{\partial p}{\partial \eta}=-M\left(u\frac{\partial v}{\partial \xi}+v\frac{\partial v}{\partial \eta}\right)+H\left[\frac{1}{3}\frac{\partial^2 u}{\partial \xi \partial \eta}+\frac{\partial^2 v}{\partial \xi^2}+\frac{4}{3}\frac{\partial}{\partial \eta}\left(\frac{1}{\eta}\frac{\partial}{\partial \eta}(\eta v)\right)\right] \tag{3}$$

The dimensionless variables are choose as $u = u'/u_0$, u' = axial velocity, u_0 = initial mean velocity; $v = v'/u_0$, v' = radial velocity; $p = (p'-p_e')/\rho_0 u_0 a_0$, p' = pressure, p_e' = initial pressure at valve, ρ_0 = mean density of the liquid, a_0 = wave speed; $\xi = x/R$, x = axial distance along pipe centerline, R = radius of the pipe; $\eta = r/R$, r = radial distance from pipe centerline; and $\tau = a_0 t/R$, t = time. Dimensionless parameters $M = u_0/a_0$; $H = \nu/Ra_0$, ν = kinematic viscosity of the liquid.

2.2. Original Mitra-Rouleau scheme

Mitra and Rouleau developed an implicit factorization method for solving numerically the above-mentioned full-2D water hammer model [6]. More specifically, the two-dimensional problem was decomposed into two one-dimensional problems. They firstly swept in the axial direction and solved the equations (4a), (4b) and (4c) to get p^{*n+1}, u^{*n+1} and v^{*n+1}, and then swept in the radial direction and solved the equations (5a), (5b) and (5c) to get p^{n+1}, u^{n+1} and v^{n+1}.

$$p_{i,j}^{*n+1} + \frac{1}{3}\Delta\tau(\frac{\partial u^{*n+1}}{\partial \xi})_{i,j}^{+} + \frac{1}{3}\Delta\tau(\frac{\partial u^{*n+1}}{\partial \xi})_{i,j}^{-} + \frac{1}{3}\Delta\tau(\frac{\partial p^{*n+1}}{\partial \xi})_{i,j}^{+} - \frac{1}{3}\Delta\tau(\frac{\partial p^{*n+1}}{\partial \xi})_{i,j}^{-} = (T_1^n)_{i,j} \tag{4a}$$

$$u_{i,j}^{*n+1} + \frac{1}{3}\Delta\tau(\frac{\partial p^{*n+1}}{\partial \xi})_{i,j}^{+} + \frac{1}{3}\Delta\tau(\frac{\partial p^{*n+1}}{\partial \xi})_{i,j}^{-} + \frac{1}{3}\Delta\tau(\frac{\partial u^{*n+1}}{\partial \xi})_{i,j}^{+} - \frac{1}{3}\Delta\tau(\frac{\partial u^{*n+1}}{\partial \xi})_{i,j}^{-} = (T_2^n)_{i,j} \tag{4b}$$

$$v_{i,j}^{*n+1} = (T_3^n)_{i,j} \tag{4c}$$

At a given point j along the radial direction, there were three equations (4a), (4b) and (4c) for each inner axial point i, and wrote all these equations in matrix form: $\boldsymbol{A_1 z_1} = \boldsymbol{b_1}$, where $\boldsymbol{A_1}$ = coefficient matrix, $\boldsymbol{z_1}$ = unknown vector, $\boldsymbol{b_1}$ = known vector.

$$p_{i,j}^{n+1} + \frac{1}{3}\Delta\tau(\frac{\partial v^{n+1}}{\partial \eta})_{i,j}^{+} + \frac{1}{3}\Delta\tau(\frac{\partial v^{n+1}}{\partial \eta})_{i,j}^{-} + \frac{2}{3}\Delta\tau(\frac{v^{n+1}}{\eta})_{i,j} + \frac{1}{3}\Delta\tau(\frac{\partial p^{n+1}}{\partial \eta})_{i,j}^{+} - \frac{1}{3}\Delta\tau(\frac{\partial p^{n+1}}{\partial \eta})_{i,j}^{-} = p_{i,j}^{*n+1} \tag{5a}$$

$$u_{i,j}^{n+1} = u_{i,j}^{*n+1} \tag{5b}$$

$$v_{i,j}^{n+1} + \frac{1}{3}\Delta\tau(\frac{\partial p^{n+1}}{\partial \eta})_{i,j}^{+} + \frac{1}{3}\Delta\tau(\frac{\partial p^{n+1}}{\partial \eta})_{i,j}^{-} + \frac{1}{3}\Delta\tau(\frac{\partial v^{n+1}}{\partial \eta})_{i,j}^{+} - \frac{1}{3}\Delta\tau(\frac{\partial v^{n+1}}{\partial \eta})_{i,j}^{-} = v_{i,j}^{*n+1} \tag{5c}$$

At a given point i along the axial direction, there were three equations (5a), (5b) and (5c) for each inner radial point j, and wrote all these equations in matrix form: $\boldsymbol{A_2 z_2} = \boldsymbol{b_2}$, where $\boldsymbol{A_2}$ = coefficient matrix, $\boldsymbol{z_2}$ = unknown vector, $\boldsymbol{b_2}$ = known vector.

2.3. Modified Mitra-Rouleau scheme

In this study, the original coefficient matrix $\boldsymbol{A_1}$ is transferred into one tri-diagonal matrix, equation (6), which can be solved by Gaussian elimination method efficiently.

$$\begin{pmatrix} 1 & C_1 & & & & & & 0 \\ \frac{L^2+M^2}{M^2-L^2} & 1 & \frac{2ML}{L^2-M^2} & & & & & \\ & \frac{2ML}{M^2-L^2} & 1 & \frac{L^2+M^2}{L^2-M^2} & & & & \\ & & \ddots & \ddots & \ddots & & & \\ & & & \ddots & \ddots & \ddots & & \\ & & & & \frac{2ML}{M^2-L^2} & 1 & \frac{2ML}{L^2-M^2} & \\ & & & & & \frac{2ML}{M^2-L^2} & 1 & \frac{L^2+M^2}{L^2-M^2} \\ 0 & & & & & & C_2 & 1 \end{pmatrix} \tag{6}$$

Similarly, the original coefficient matrix $\boldsymbol{A_2}$ is transferred into the other tri-diagonal matrix, equation (7).

$$\begin{pmatrix} 1 & C_3 & & & & & & 0 \\ \frac{W_2Y-Z^2}{Y^2-Z^2} & 1 & \frac{YZ+X_3Z}{Y^2-Z^2} & & & & & \\ & \frac{YZ-W_2Z}{W_2X_3+Z^2} & 1 & \frac{W_2Y-Z^2}{W_2X_3+Z^2} & & & & \\ & & \ddots & \ddots & \ddots & & & \\ & & & \ddots & \ddots & \ddots & & \\ & & & & \frac{W_{J-2}Y-Z^2}{Y^2-Z^2} & 1 & \frac{YZ+X_{J-1}Z}{Y^2-Z^2} & \\ & & & & & \frac{YZ-W_{J-2}Z}{W_{J-2}X_{J-1}+Z^2} & 1 & \frac{W_{J-2}Y-Z^2}{W_{J-2}X_{J-1}+Z^2} \\ 0 & & & & & & C_4 & 1 \end{pmatrix} \tag{7}$$

Where C, L, M, W, X, Y and Z are coefficients depending on $\Delta\xi$, $\Delta\eta$ and $\Delta\tau$.

2.4. Initial and boundary conditions

The modified Mitra-Rouleau scheme is extended to a reservoir-pipe-valve experimental system, with following typical initial and boundary conditions:

- Initial condition (Poiseuille laminar flow)

$$u = 2\left(\eta^2 - 1\right);\ v = 0;\ p = 8H\xi \text{ at } \tau = 0 \tag{8}$$

- Boundary conditions (pipe centerline, pipe wall and reservoir)

$$\frac{\partial u}{\partial \eta} = 0;\ v = 0;\ \frac{\partial p}{\partial \eta} = 0 \text{ at } \eta = 0 \tag{9}$$

$$u = 0;\ v = 0;\ \frac{\partial p}{\partial \eta} = R_3 \text{ at } \eta = 1 \tag{10}$$

$$\frac{\partial u}{\partial \xi} = R_1;\ v = 0;\ p = 8H\xi \text{ at } \xi = 1 \tag{11}$$

- Valve operations (incident wave)

$$u = 2\left(\eta^2 - 1\right) \text{ when } \tau = 0,\ u = 0 \text{ when } \tau > 0;\ \frac{\partial p}{\partial \xi} = -\frac{\partial u}{\partial \tau} + R_2 \text{ (Suddenly valve closure)} \tag{12}$$

$$u = 0.5 \cdot \left[2\left(\eta^2 - 1\right)\right] \cdot \left[\cos\left(2\pi f_{in}\tau\right) + 1\right] \text{ when } \tau < \tau_0,\ u = 0 \text{ when } \tau > \tau_0;\ \frac{\partial p}{\partial \xi} = -\frac{\partial u}{\partial \tau} + R_2 \text{ (Perturbation)} \tag{13}$$

3. Results and discussions

3.1. Test cases

The full-2D model is applied to a classical reservoir-pipe-valve water hammer experimental system (Fig. 1). Initially, keeps the downstream valve fully open, and the steady laminar flow in the pipe has an average velocity u_0. The transients are caused by different operations on the downstream valve. Three test cases (Test No. 1, 2 and 3), with different numerical test parameters (Table 1), are investigated in this research. Test No. 4 and 5 are investigated in the same experimental system except for the different operations on the downstream valve. Note that the fluid properties and initial conditions are similar to the study of Mitra and Rouleau [6] for convenient comparison.

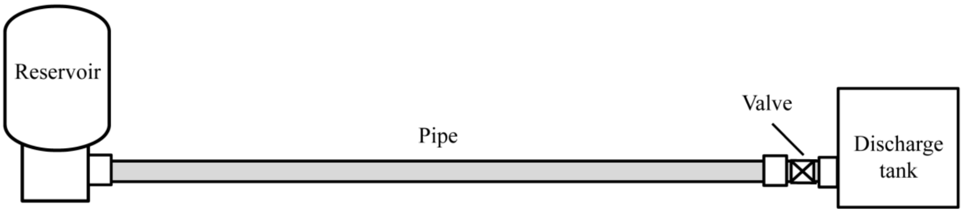

Fig. 1. Sketch of a reservoir-pipe-valve experimental system.

Table 1. Parameters for test cases used in transient laminar pipe flow.

Test No.	L/R	Reynolds No.	Wave speed (m/s)	Kinematic viscosity (m^2/s)	$T(s)$	$d\xi=d\eta=d\tau$	Valve operation
1	80	100	1325	3.97e-05	0.02	0.02	Suddenly close
2	80	1000	1325	3.97e-05	0.02	0.02	Suddenly close
3	160	100	1325	3.97e-05	0.04	0.02	Suddenly close
4	80	1000	1325	3.97e-05	0.02	0.02	Perturbation f_{in1}
5	80	1000	1325	3.97e-05	0.02	0.02	Perturbation f_{in2}

3.2. Results and discussions

- Model validation

In spite of the large amount of literature on transient laminar pipe flows, the experimental data on two-dimensionality of laminar transients is still relatively deficient due to the difficulty of measuring those data in experiments. To validate the presented full-2D water hammer model, the results of averaged pressure head across the pipe area at different locations along the pipeline are compared with the numerical data of Zielke's 1D analytical model, which has been validated through the experimental test data [7].

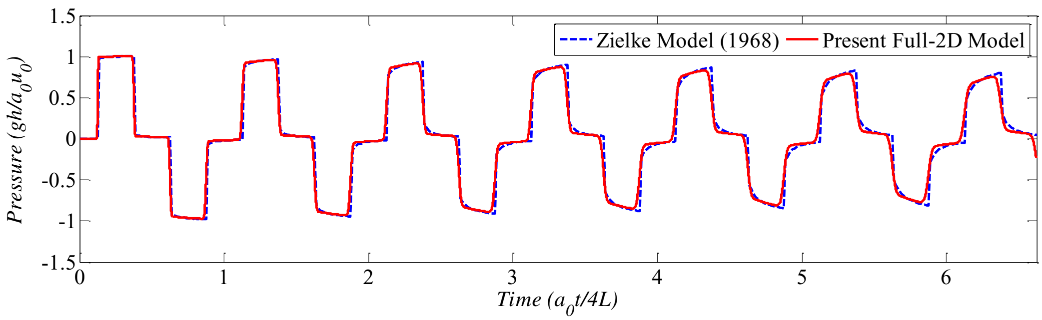

Fig. 2. Pressure history at the pipe mid-length, L/R = 80, Re = 100 (Test No. 1).

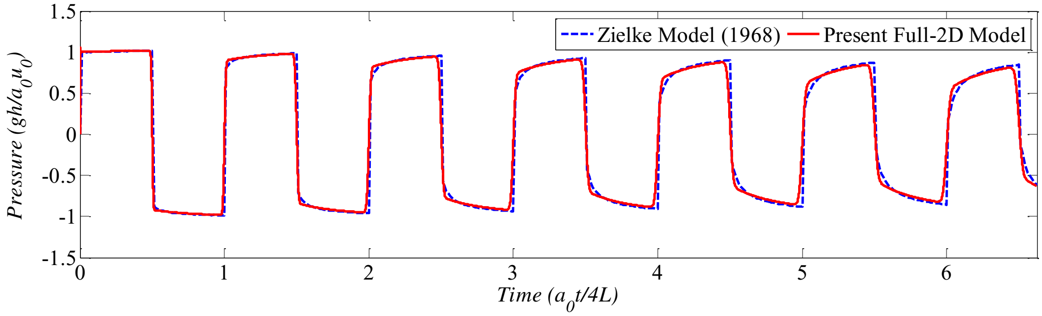

Fig. 3. Pressure history at the downstream valve, L/R = 80, Re = 1000 (Test No. 2).

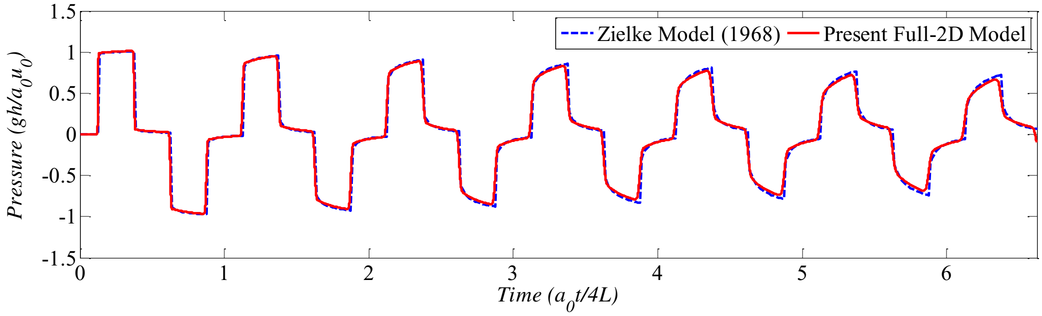

Fig. 4. Pressure history at the pipe mid-length, L/R = 160, Re = 100 (Test No. 3).

The pressure responses in the time domain for Tests No. 1, 2 and 3 are shown in Figs. 2, 3 and 4. The pressure is normalized by the steady state pressure head at the downstream valve, and time is normalized by the system period $T = a_0t/4L$. Good agreement between full-2D model and Zielke's model in both pressure amplitude and pressure phase could be seen in Test No. 1, 2 and 3, which demonstrates the validity of presented full-2D model for transient laminar pipe flows. For illustration, Test No. 3 with Re = 1000 is used for further analysis and discussion. Different incident wave conditions, which are defined by the ratio of incident wave frequency (f_{in}) and radial wave frequency ($f_r \sim= a_0/4R^*$, $R^* = 0.4R$), are investigated in the following study.

- Low frequency wave test ($f_{in}/f_r << 1$)

Under the condition of fast downstream valve closure in Fig. 1, the temporal variations of pressure at the valve for three typical radial points (Test No. 2) are plotted in Fig. 5. Note that the worst-case moment for plane wave assumption is observed within the short interval after valve closure. Fig. 5 also shows that the pressure at pipe centerline (η = 0.0) reaches the peak value of almost 2.0 when the downstream valve is completely closed at time τ = 0.0. This value is almost double that of cross sectional average pressure at time τ = 0.0 in Fig. 5, because the axial velocity at pipe centerline is twice the value of cross sectional average velocity. This result is consistent with the study [6]. After this short period, the four pressure curves are almost indistinguishable. That is to say, the radial pressure change at downstream valve is not evident in the rest of the time.

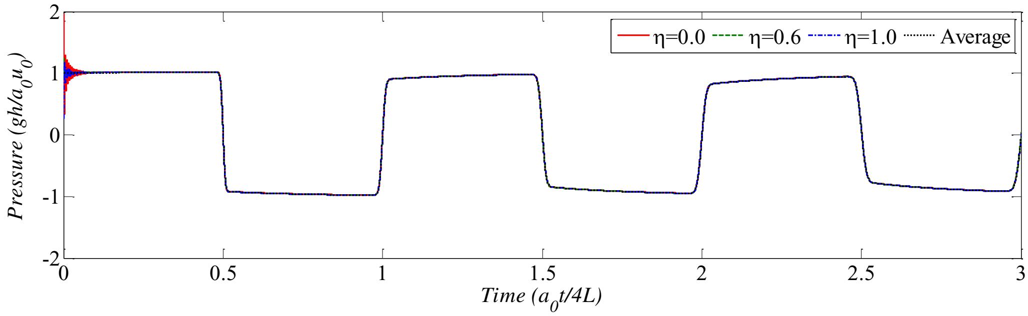

Fig. 5. Pressure history of three radial points at the downstream valve, *L/R* = 80, *Re* = 1000 (Test No. 2).

- High frequency wave test (f_{in1}/f_r ~= 0.2 < 1)

Under this condition, the HFW during 0-0.5 a_0/L in Test No. 4 is generated by periodically repeating the close-open process of downstream valve, and the axial velocity profile at downstream valve is given by $u_1 = 0.5\cdot[2(\eta^2-1)]\cdot[cos(2\pi f_{in1}\tau)+1]$. The temporal variations of pressure at downstream valve for three different radial points are plotted in Fig. 6. As is shown in Fig. 6, the wave generated at the downstream valve during the time period 0-0.5a_0/L is plane wave. This can be attributed to the relative low value of f_{in1} compared with radial pressure wave frequency f_r, which gives enough time to radial pressure wave propagating in the whole cross section of pipe before the total closure of downstream valve. During the short period after valve closure at $\tau = 0.5L/a_0$, the plane wave assumption experiences the worst-case moment, which is very similar to that of Test No. 2. After this short period, all three pressure curves are almost indistinguishable from the average pressure curve, which confirm the validity of plane wave assumption in the rest of the time. The amplitude of the HFW is dissipated evidently as it travels back and forth in the pipe.

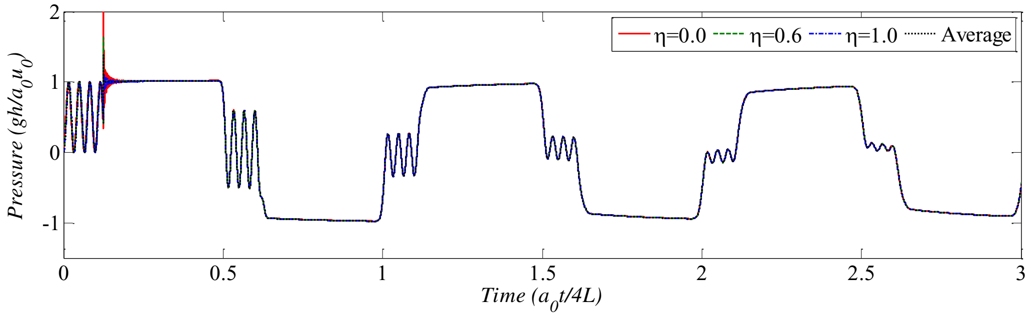

Fig. 6. Pressure history of three radial points at the downstream valve, *L/R* = 80, *Re* = 1000 (Test No. 4).

- Extremely high frequency wave test (f_{in2}/f_r ~= 4 >> 1)

The generation mechanism of extremely HFW (f_{in2}/f_r ~= 4) is the same as that of Test No. 4, and the axial velocity profile at downstream valve is given by $u_2 = 0.5\cdot[2(\eta^2-1)]\cdot[cos(2\pi f_{in2}\tau)+1]$ with an extreme frequency of wave injection. The temporal variations of pressure at the downstream valve for three different radial points are plotted in Fig. 7, which clearly shows that the radial variation of pressure at the downstream valve during the time period 0-0.5a_0/L is very evident. This is due to the relative large value of f_{in2} compared with radial pressure wave frequency f_r so that there is no enough time for the radial pressure wave to influence the pressure profile across the pipe area to become plane wave. At $\tau = 0.5L/a_0$, the valve is totally closed, and the pressure response shortly after valve closure is similar with that of Test No. 2 and No. 4. However, compared to the results of Test No. 4 in Fig. 6, the generated HFW is dissipated rapidly as it propagates along the pipeline in the system, such that these very high frequent oscillations disappear completely (i.e., became plane wave again) when the wave is reflected back from the upstream to the transient source location. These evidences again indicate that the radial wave propagation (in both dispersion and dissipation) could have potentially important influence on the HFW propagation. Therefore, it should be very careful to extremely increase the incident wave frequency for the pipeline assessment.

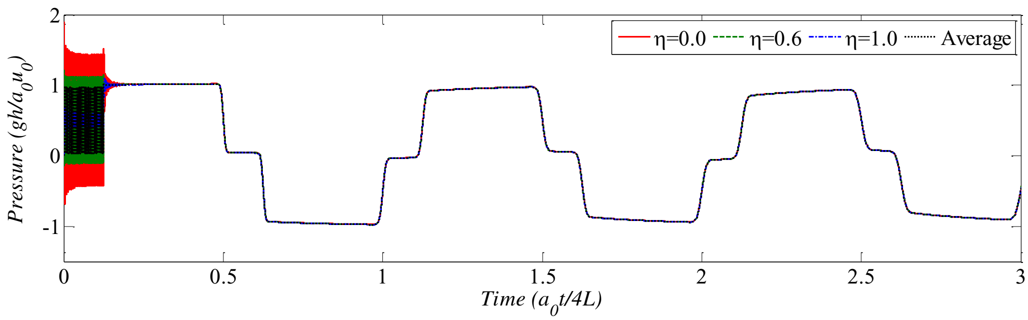

Fig. 7. Pressure history of three radial points at the downstream valve, L/R = 80, Re = 1000 (Test No. 5).

4. Conclusions

This study addresses the efficiency problem of original Mitra-Rouleau scheme for solving the full-2D water hammer model, and then the modified Mitra-Rouleau scheme is applied to a classical reservoir-pipe-valve experimental system. The validity of the modified full-2D model and scheme has been confirmed by the result comparison of averaged transient pressure head with the classical Zielke's analytical model. Finally, the plane wave assumption in transient laminar pipe flow is evaluated by full-2D water hammer model under both LFW and HFW conditions. The key conclusions are:

- The modified Mitra-Rouleau scheme is successfully applied to the reservoir-pipe-valve system, and good agreement of averaged transient pressure traces between the present full-2D model and Zielke's analytical model has been obtained from different tests.
- At the valve, the plane wave assumption is invalid during the period shortly after valve closure.
- When the perturbation frequency f_{in} at the transient source location is comparable to or larger than the radial pressure wave frequency f_r, the radial pressure change at the valve is evident during the perturbation.
- HFW has higher radial dissipation and dispersion rates compared with LFW, which reminds researchers to choose the frequency range appropriately when using the HFW for pipe system diagnosis.

The results and findings of this study may promote the understanding of the influence of plane wave assumption as well as the utilization of LFW and HFW for the development of transient-based pipe faults detection technologies.

Acknowledgements

This paper was supported by the research grants from: (1) Hong Kong Polytechnic University (HKPU) under projects with numbers 1-ZVGF, 3-RBAB, G-YBC9 and G-YBHR; and (2) Hong Kong Research Grant Council (RGC) under the project no. T21-602/15-R.

References

[1] M.H. Chaudhry, Applied hydraulic transients, Van Nostrand Reinhold, New York, 1979.
[2] M.S. Ghidaoui, M. Zhao, D.A. McInnis, D.H. Axworthy, A review of water hammer theory and practice, Appl. Mech. Rev. 58.1 (2005) 49-76.
[3] A.E. Vardy, K.L. Hwang, A characteristics model of transient friction in pipes, J. Hydraul. Res. 29.5 (1991) 669-684.
[4] G. Pezzinga, Quasi-2D model for unsteady flow in pipe networks, J. Hydraul. Eng. 125.7 (1999) 676-685.
[5] P.J. Lee, H.F. Duan, M.S. Ghidaoui, B.W. Karney, Frequency domain analysis of pipe fluid transient behaviour, J. Hydraul. Res. 51.6 (2013) 609-622.
[6] A.K. Mitra, W.T. Rouleau, Radial and axial variations in transient pressure waves transmitted through liquid transmission lines, J. Fluids Eng. 107.1 (1985) 105-111.
[7] W. Zielke, Frequency-dependent friction in transient pipe flow, J. Fluids Eng. 90.1 (1968) 109-115.